Helium clustering in neutron-rich Be isotopes

N.I. Ashwood, M. Freer, Mohamed-Salem Ahmed, J.C. Angélique, V. Bouchat,
W.N. Catford, N.M. Clarke, N. Curtis, O. Dorvaux, B.R. Fulton, et al.

Helium clustering in neutron-rich Be isotopes

N.I. Ashwood [a], M. Freer [a], S. Ahmed [a], J.C. Angélique [b], V. Bouchat [c], W.N. Catford [d,b],
N.M. Clarke [a], N. Curtis [a], O. Dorvaux [e], B.R. Fulton [f], F. Hanappe [c], Y. Kerckx [c],
M. Labiche [g], J.L. Lecouey [b,1], R.C. Lemmon [h], F.M. Marqués [b], T. Materna [c],
A. Ninane [i], G. Normand [b], N.A. Orr [b], S. Pain [d], N. Soić [a,2], L. Stuttgé [e], C. Timis [b,3],
A. Unshakova [j], J.S. Winfield [k], V.A. Ziman [a]

[a] School of Physics and Astronomy, University of Birmingham, Edgbaston, Birmingham, B15 2TT, United Kingdom
[b] Laboratoire de Physique Corpusculaire, ISMRA and Université de Caen, IN2P3-CNRS, 14050 Caen Cedex, France
[c] Université Libre de Bruxelles, CP 226, B-1050 Bruxelles, Belgium
[d] School of Electronics and Physical Sciences, University of Surrey, Guildford, Surrey, GU2 7XH, United Kingdom
[e] Institut de Recherches Subatomique, IN2P3-CNRS/Université Louis Pasteur, BP 28, 67037 Strasbourg Cedex, France
[f] Department of Physics, University of York, Heslington, York, YO10 5DD, United Kingdom
[g] Department of Electronic Engineering and Physics, University of Paisley, Paisley, PA1 2BE, United Kingdom
[h] CLRC Daresbury Laboratory, Daresbury, Warrington, Cheshire, WA4 4AD, United Kingdom
[i] Institut de Physique, Université Catholique de Louvain, Louvain-la-Neuve, Belgium
[j] Joint Institute for Nuclear Research, 141980 Dubna, Moscow Region, Russia
[k] Instituto Nazionale di Fisica Nucleare, Laboratori Nazionali del Sud, 44-95123 Catania, Italy

Abstract

Measurements of the helium-cluster breakup and neutron removal cross-sections for neutron-rich Be isotopes $^{10-12,14}$Be are presented. These have been studied in the 30 to 42 MeV/nucleon energy range where reaction measurements are proposed to be sensitive to the cluster content of the ground-state wave-function. These measurements provide a comprehensive survey of the decay processes of the Be isotopes by which the valence neutrons are removed revealing the underlying α–α core-cluster structure. The measurements indicate that clustering in the Be isotopes remains important up to the drip-line nucleus ^{14}Be and that the dominant helium-cluster structure in the neutron-rich Be isotopes corresponds to α–Xn–α.
© 2003 Published by Elsevier B.V. Open access under CC BY license.

E-mail address: n.i.ashwood@bham.ac.uk (N.I. Ashwood).

[1] Present address: NSCL, Michigan State University, Michigan 48824, USA.
[2] Present address: Rudjer Bošković Institute, Bijenička 54, HR-10000 Zagreb, Croatia.
[3] Present address: School of Electronics and Physical Sciences, University of Surrey, Surrey, GU2 7XH, United Kingdom.

The structure of nuclear matter at the limits of stability has always been a source of fascination. These limits are bounded by the extremes of excitation energy or spin, on one hand, and by the extremes of either total number of nucleons or ratios of protons to neutrons (isospin) on the other. Most notably, radioactive beam facilities provide access to the limit of neutron excess. Here, structural properties are known to differ from normal nuclear matter, as they are strongly influenced by the weak binding of the valence neutrons. The classic example is the halo, where weakly bound neutrons exist as a diffuse cloud around a compact core [1]. In this case there is a decoupling of the valence neutrons from a core, or cluster, of normal nuclear matter.

Recently, it has been speculated that such clustering may be a general feature of drip-line nuclei caused by the tendency of the nucleus to distribute the neutron excess among the core nucleons [2]. In order to maximize the overlap of the excess neutrons with protons, the core may either deform, enhancing the surface area, or, optimally, form clusters. Thus, the ground states of neutron drip-line nuclei may resemble clusters embedded in a cloud of weakly bound neutrons. This possibility presents a departure from the conventional picture of clustering in light nuclei where cluster structure appears at excitation energies which coincide with cluster decay thresholds [3]. In the case of these neutron-rich nuclei the cluster decay thresholds lie at relatively high excitation energies, and thus this requires a new approach to understand these nuclei.

Certain nuclei already possess a predisposition towards clustering. For example, ^{8}Be clearly demonstrates a strong α–α cluster character [4,5]. Recent experimental and theoretical developments indicate that this underlying cluster structure has a strong influence on the neutron-rich Be isotopes. In particular, the two-centered nature of the potential in which the valence neutrons reside may produce molecular type characteristics in these nuclei [6,7]. Calculations using the anti-symmetrized molecular dynamics (AMD) framework suggest such features can occur in the Be isotopes [8,9]. The same model predicts that the normally compact boron isotopes become highly clustered at the drip-line [10], in line with the ideas concerning the optimization of the proton–valence-neutron overlap [2].

Direct access to such structural properties of the ground states of very neutron-rich nuclei is extremely challenging due to the fact that the ^{x}He cluster breakup thresholds increase significantly towards the drip-line. However, given that the breakup process proceeds from states inelastically excited above the helium decay threshold, and that states close to decay thresholds typically possess large cluster content [3], then the breakup process should be sensitive to the cluster structure in the ground state via the overlap of the ground state and excited state. It is possible also that the breakup process may be direct rather than resonant. However, measurements of the breakup of ^{12}Be [11] indicate that the resonant component is dominant. Moreover, measurements of the direct breakup of halo nuclei demonstrate that there is a strong dependence on the halo structure of the ground state wavefunction. Similarly, there should be some sensitivity to the cluster structure of the ground state in the direct breakup process. Indeed, the AMD model has been used to explore how the fragmentation of beams of boron isotopes may be used to extract a signature for the clustering in the ground state [12]. This study revealed that such clustering may be probed via fragmentation if energies in the region of 30 MeV/nucleon were used. However, studies of the most neutron-rich boron isotope (^{19}B), as suggested in [12], is beyond the capability of present day experimental facilities. It is, however, possible to study the beryllium nuclei all the way from stability to the drip-lines. Here we present comprehensive measurements of ^{x}He-cluster, which were explored theoretically for the boron isotopes, and neutron breakup cross-sections for the beryllium isotopes $A = 10$, 11, 12 and 14. These data should provide a significant test of our understanding of the structure of nuclei at the neutron drip-line.

The measurements were performed at the GANIL accelerator facility with the production of ^{10,11,12,14}Be secondary beams via the fragmentation of ^{13}C and ^{18}O primary beams. The reaction spectrometer produced beams of purity $\geqslant 95\%$ for the lighter isotopes and $\simeq 20\%$ for the heaviest and count rates of the order of 10^4 pps for masses 10, 11 and 12 (limited by the count rate capacity of the detection system) and ~ 50 pps for ^{14}Be. Identification of the beam particle was achieved using time-of-flight through the LISE separator as measured by a PPAC at the entrance to the

reaction chamber. The energies of the 4 beams were 30.9, 41.7, 41.8 and 34.4 MeV/nucleon in order of increasing mass.

The beam was tracked onto 20 to 275 mg/cm^2 carbon targets using two drift chambers, providing a measurement of the incident position and angle of the projectile. The beam and reaction products then entered a zero-degree telescope formed from two 500 μm thick, 16-strip position-sensitive silicon detectors placed 15 cm from the target. These two detectors were arranged with orthogonal strips, providing a measurement of the incident ions to ⩽ 1 mm in both the x and y directions (the z-coordinate being the beam direction). Behind the strip detectors was a close packed array of 16, 2.5 cm thick, 2.5 × 2.5 cm^2, CsI scintillators. These were placed at 30 cm from the target so as to cover the same solid angle as the strip detectors as measured from the target. Calibration of the energy response of the silicon and CsI detectors was achieved using α-sources and a mixed beam of light ions of known energy. Neutrons produced in reactions of the beam were detected using an array of ~ 100 neutron detectors (DéMoN) arranged in a similar manner to that shown in [13]. These detectors gave a single-neutron detection efficiency of $\sim 15\%$ (as in [15]). Monte Carlo simulations of the response of the charged-particle detection system indicates that the efficiency for the detection of the breakup of the Be isotopes into two ^{x}He nuclei was 40 to 50% and almost independent of excitation energy of the decaying system. The measured relative energy of the decay products ($E_{\mathrm{rel}} = \frac{1}{2}\mu v_{\mathrm{rel}}^2$) thus allowed the excitation energy to be deduced ($E_x = E_{\mathrm{rel}} + E_{\mathrm{thresh}}$). For multiplicity-2 events in the charged-particle telescopes it is necessary to correlate the events in the three sections of the telescope (silicon, silicon and CsI). This was performed utilizing the position information of each strip detector and from the physical location of each CsI detector behind the strips. Using this technique, and the ΔE–E method, it was possible to identify the mass of each of the coincident particles. Fig. 1 shows such a particle identification spectrum for these multiplicity-2 events produced using the ^{12}Be beam. The presence of well defined loci demonstrates the successful identification of both particles.

A knowledge of the breakup yields, the target thickness (and hence the number of target nuclei, N_t), detection efficiency, ϵ, and the integrated beam
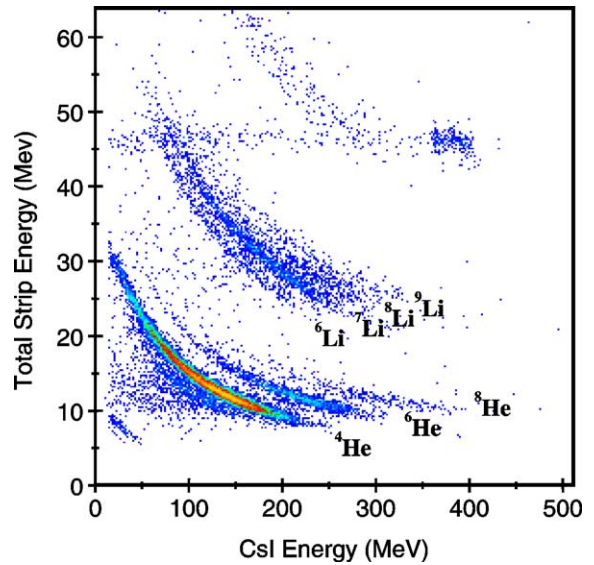

Fig. 1. Particle identification spectrum (E_{Si} versus E_{CsI}) for the zero degree detector, for the ^{12}Be beam. Note that the helium isotopes are clearly resolved and that the backgrounds are comparatively small.
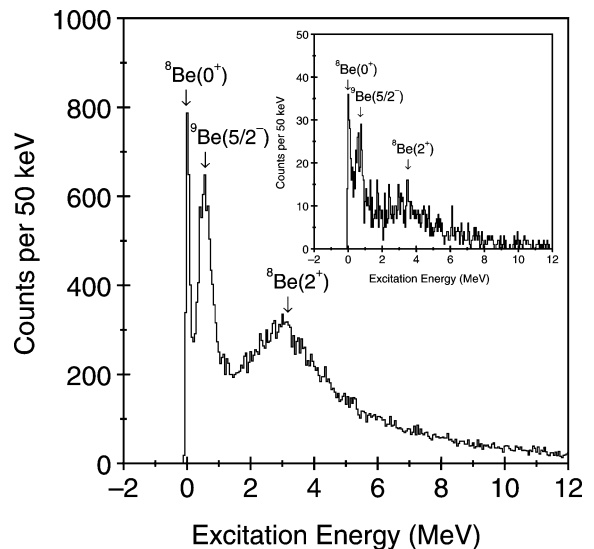

Fig. 2. The excitation energy spectrum corresponding to $\alpha + \alpha$ coincidences from the ^{12}Be beam. The peaks correspond to the decay of the ground-state (92 keV) and the first excited state (3.04 MeV, 2$^+$). The peak at ~ 600 keV is produced by the decay of the 2.43 MeV (5/2$^-$) state in ^{9}Be to the tail of the 2$^+$ state in ^{8}Be. The inset is the excitation energy spectrum corresponding to $\alpha + \alpha$ coincidences from the ^{14}Be beam.
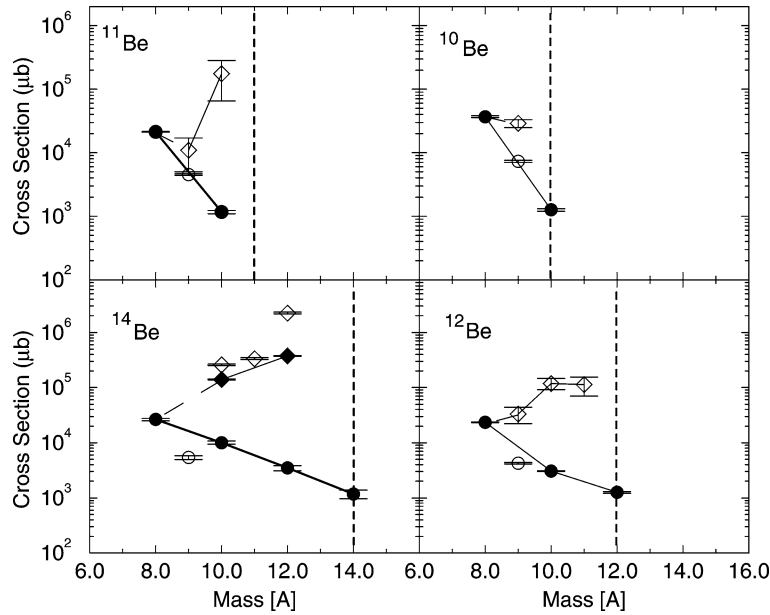
Fig. 3. Neutron-removal (open diamonds) and cluster breakup (filled circles) cross-sections for the neutron-rich Be isotopes versus the sum of the mass of the decay fragments [A]. The neutron cross-sections are normalized by dividing by the difference in the number of neutrons between the observed fragment and the projectile, i.e., x as described in the text. For ^{14}Be the filled diamonds correspond to the measurements of [14,15]. Note, the points for the ^{9}Be breakup (open circles) are lower limits deduced from the 600 keV peak in the ^{8}Be spectrum in Fig. 2. The vertical dotted lines indicate the mass of the projectile. The cross-sections are listed in Tables 1 and 2.

exposure, N_b, allowed the cross-sections, σ, for the various breakup processes to be calculated using Eq. (1)

$$\sigma = \frac{\text{Yield}}{\epsilon N_t N_b}. \tag{1}$$

Analysis of target-out runs show that no contribution to the yield is obtained from reactions within either the strip or CsI detectors. In addition, as noted above, it was possible to deduce the excitation energy of the decaying system. As an example, Fig. 2 shows the ^{4}He + ^{4}He invariant mass spectrum (E_x) for the ^{12,14}Be beams. It is clear that a large fraction of the events involving the dissociation of ^{14}Be (^{12}Be) proceed via 6 (4) neutron emission to form ^{8}Be, i.e., the decay process does not always follow from the decay into neutron-rich helium isotopes followed by neutron emission, i.e., unbound excited states of ^{x}He. The evidence for this is the observation of peaks in the ^{8}Be excitation energy spectrum at energies which correspond to the decay of the ground-state (92 keV) and the first excited state (3.04 MeV, 2^+). There is one further feature in this spectrum, at ~ 600 keV,

which does not correspond to a resonance in ^{8}Be but is produced by the decay of the 2.43 MeV ($5/2^-$) state in ^{9}Be to the tail of the 2^+ state in ^{8}Be. The presence of this feature suggests a fraction of the yield proceeds via sequential 6n emission to ^{8}Be. Similar features are also present in the ^{4}He + ^{4}He decay spectra measured with the other Be projectiles.

The mass identification provided by the zero degree telescope allows the resolution of all the He isotopes and thus permits all stages of the decay process to be reconstructed. For example, in the case of ^{14}Be it is possible to reconstruct the decay into ^{8}He + ^{6}He, or following the emission of neutrons from the projectile, the decay of ^{12}Be* into ^{6}He + ^{6}He (or ^{4}He + ^{8}He), or the decay of ^{10}Be* to ^{6}He + ^{4}He, or, finally, as discussed above, ^{8}Be to ^{4}He + ^{4}He. The cross-sections for these processes are plotted in Fig. 3. These cross-sections are also presented in Table 1, with the cross-sections for ^{x}Be + 1n (i.e., core fragment plus one neutron) decay in Table 2. We note that the efficiency for multi-neutron detection was prohibitively small, and thus these channels are not presented. The neutron cross-sections have been calculated by selecting

Table 1
Cross-sections measured for He-cluster breakup, in units of mb

	^{6}He + ^{8}He (mb)	^{6}He + ^{6}He (mb)	^{8}He + ^{4}He (mb)	^{6}He + ^{4}He (mb)	^{4}He + ^{4}He (mb)			Total (mb) He + He
					^{8}Be$_{gs}$	^{9}Be(5/2$^-$)	^{8}Be(2$^+$)	
^{14}Be	1.17(0.20)	1.33(0.22)	2.15(0.30)	10.04(0.65)	4.40(0.41)	5.40(0.44)	16.61(1.19)	41.09(1.54)
^{12}Be		0.23(0.02)	1.02(0.04)	3.04(0.05)	2.89(0.10)	4.25(0.10)	16.42(0.37)	27.86(0.40)
^{11}Be				1.17(0.07)	3.59(0.14)	4.52(0.11)	13.12(0.31)	22.40(0.36)
^{10}Be				1.14(0.05)	7.97(0.40)	7.32(0.30)	21.6(1.1)	42.68(0.68)

beam velocity neutrons ($E_n > 0.37 E_{beam}/A$). In the case of ^{11,12}Be these were calculated by integrating the neutron angular distributions with a Lorentzian single neutron line-shape, whilst subtracting the background from reactions producing neutrons (then detected in the DéMoN array), within the CsI component of the telescopes, as deduced from measurements with no target [15]. In the case of ^{10,14}Be data no background measurements were performed and thus the cross-sections provide upper limits only. For ^{14}Be, measurements of these cross-sections, including the background subtraction, have already been made by Labiche et al. [14,15] at 35 MeV/u, and these are also shown in Table 2. Given an analysis of the no target yield from the ^{12}Be data ($\sim$ 20–30% of events in the 2n removal channel are from the target) the cross-sections are consistent. Comparison of the cross-sections with earlier studies show reasonable agreement. The 0.18(0.11) b cross-section for the removal of 1n from ^{11}Be compares with that extracted by Anne et al. [16] of 0.12(0.02) b, and the 0.11(0.04) b 1n removal cross-section from ^{12}Be is in close agreement with that measured by Navin et al. [17], 0.045(0.005) b, albeit at 78 MeV/u. Similar agreement is found with the helium breakup measurements reported in [18].

The measurement of the multi-neutron removal channels via the detection of the core plus one neutron presents the advantage that the detection efficiency does not become prohibitively small. Naively, the true cross-section for the $A-Xn$ channel should be reduced by a factor X in order to correct for the larger detection efficiency for these channels. However, the neutron angular distributions vary slightly from decay step to decay step and thus the efficiency is not constant (there is a 17% change in the angular distributions between one, two and three neutron removal from ^{12}Be). Moreover, the multiplicity of the emitted neutrons does not necessarily equal the number of missing

Table 2
Cross-sections measured for observed fragment in coincidence with a single neutron, in units of mb. Note in the case of ^{10,14}Be the neutron cross-sections provide upper limits. The row marked ^{14}Be† are the background subtracted cross-sections from [14,15]

	^{12}Be (mb)	^{11}Be (mb)	^{10}Be (mb)	^{9}Be (mb)
^{14}Be	2248(82)	670(23)	799(26)	
^{14}Be†	750(10)		420(10)	
^{12}Be		113(43)	237(54)	100(35)
^{11}Be			175(110)	22(12)
^{10}Be				29(4)

neutrons, with the possibility of projectile neutrons interacting strongly with the target [15]. Indeed, the measured neutron multiplicities for ^{14}Be $\rightarrow$ ^{12}Be and ^{14}Be $\rightarrow$ ^{10}Be are found to be 1.63(0.26) and 2.9(0.8) [14,15]. Although the uncertainties are large these multiplicities indicate that there is a tendency for there to be slightly less neutrons in the final state than anticipated. Nevertheless, for the sake of the comparison with the measured helium breakup cross-sections the $^{A-X}$Be + 1n cross-sections are plotted in Fig. 3 divided by X, thus indicating the strength with which the bound states of the $A-Xn$ nucleus are populated. It should be noted that the measured neutron angular distributions for the multi-neutron removal channels are and average over those for each step.

Fig. 4 shows the mass dependence of the cluster decay cross-sections. It is not possible to plot the data for ^{11}Be in this instance as the main decay channels ^{5}He + ^{6}He and ^{4}He + ^{7}He lead to a ^{4}He + n + ^{6}He final state which cannot be unambiguously distinguished from neutron removal followed by α-decay of ^{10}Be. Figs. 4(a) and (b) show the cross-sections for the helium cluster breakup of the projectile (first-chance breakup), i.e., ^{14}Be $\rightarrow$ ^{6}He + ^{8}He, ^{12}Be $\rightarrow$ ^{6}He + ^{6}He, ^{12}Be $\rightarrow$ ^{4}He + ^{8}He, ^{10}Be $\rightarrow$ ^{6}He + ^{4}He, and
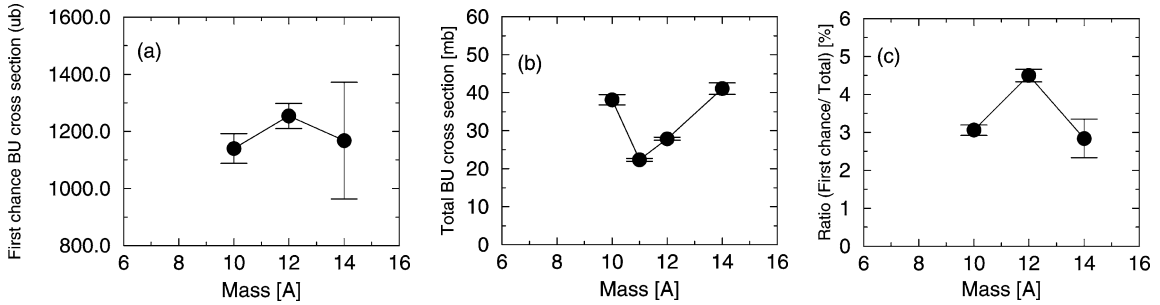
Fig. 4. (a) The first-chance cluster breakup cross-sections, i.e. $^{14}Be \rightarrow {}^{6}He + {}^{8}He$, $^{12}Be \rightarrow ({}^{6}He + {}^{6}He$ and $^{4}He + {}^{8}He)$ and $^{10}Be \rightarrow {}^{6}He + {}^{4}He$, (b) the total He + He breakup cross-sections and (c) the ratio of the first-chance breakup cross-sections to the total breakup cross-section, versus the mass of the projectile [A].

Table 3
Energy thresholds for cluster and neutron decay in units of MeV

	Neutron removal (MeV)						He + He cluster decay (MeV)	
	1n	2n	3n	4n	5n	6n		
^{14}Be	2.97	1.12	4.29	4.79	11.60	13.27	$^{6}He + {}^{8}He$	9.09
^{12}Be	3.17	3.67	10.48	12.15			$^{4}He + {}^{8}He$	8.95
^{11}Be	0.50	7.32	8.98				$^{5}He + {}^{6}He$	8.81
^{10}Be	6.81	8.48					$^{4}He + {}^{6}He$	7.41

the total He + He breakup cross-section, respectively. From the energy thresholds for $^{x}He + {}^{A-x}He$ cluster decay (Table 3) one may expect that the first-chance cross-sections for the Be isotopes would decrease with increasing mass. However, from the present data it can be seen that the first-chance breakup cross-sections are, within experimental error, mass independent. Based on the assumption that the breakup process samples the overlap between the wavefunctions of the ground state and excited states above the cluster decay threshold, these data would suggest that the di-cluster content of the nuclei does not decrease from ^{10}Be through to ^{14}Be. Indeed, as the decay thresholds do decrease, the present data may indicate that the cluster content has a slight increase with mass. The total breakup cross-section for $A = 10$, 11, 12 and 14, does however, show a strong minimum at $A = 11$ increasing to maximum values for ^{10}Be and ^{14}Be and hence the ratio of first chance to total cluster breakup reveals a maximum at $A = 12$ (Fig. 4(c)).

Early calculations of the degree of clustering in the beryllium isotopes using the AMD framework indicated a decrease in clusterization from ^{8}Be to ^{12}Be with a small increase for ^{14}Be [9], with something

like a factor of 2 change predicted in the clusterization between the ground states of ^{10}Be and ^{12}Be. However, most recent studies using this framework now indicate low-lying states possess strong cluster symmetries [19]. If, as suggested by the AMD calculations for the reactions with the boron isotopes, the breakup process is strongly influenced by the overlap of the cluster content of the ground state and that of excited states above the decay threshold, then the present measurements indicate that there is no change in the degree of clustering in the mass range 10 to 14.

By far the most dominant He-cluster breakup channel is that corresponding to the removal of all of the valence neutrons leaving the α–α core (Fig. 3). Table 3 shows the energy thresholds for $^{8}Be + Xn$ and first-chance He-cluster breakup. Remarkably, even though the thresholds for removing all valence neutrons are higher in energy, it is this channel which dominates, suggesting a strong influence of the α–Xn–α structure. Such a result cannot be explained by decay phase-space alone, in which the ^{8+Xn}Be nucleus directly dissociates into $Xn + {}^{8}Be$. The decay phase-space, calculated using the Fermi breakup model [20–22], for the breakup of $^{12,14}Be$ into the various n-body partitions at

Table 4

Calculated percentage yields for the various breakup channels for ^{12,14}Be nuclei for decays to ground states. The calculations are based on the Fermi breakup model [20–22] in which the n-body phase-space is calculated and have been performed for an excitation energy of 15 MeV. The yields are shown as a percentage of the totals for the all calculated channels

^{12}Be		^{14}Be	
^{4}He + ^{8}He	36.0	^{4}He + ^{8}He	50.2
^{6}He + ^{6}He	19.3	^{6}He + ^{6}He + 2n	0.019
^{4}He + ^{6}He + 2n	0.027	^{4}He + ^{6}He + 4n	5.10×10^{-8}
^{11}Be + 1n	40.9	^{13}Be + 1n	43.2
^{10}Be + 2n	3.7	^{12}Be + 2n	6.4
^{9}Be + 3n	0.028	^{11}Be + 3n	0.40
^{8}Be + 4n	3.4×10^{-6}	^{10}Be + 4n	0.003
		^{9}Be + 5n	7.4×10^{-8}
		^{8}Be + 6n	5.2×10^{-14}

an excitation energy of 15 MeV are shown in Table 4, and are plotted in Fig. 5 for ^{14}Be for an excitation energy of 20 MeV. It is clear that phase-space cannot account for the observed experimental trend and indeed that the opposite behavior is predicted. Moreover, in the case of ^{14}Be the decay threshold for 6n emission lies 4.2 MeV higher than that for cluster decay, and inelastic excitation probabilities would be expected to decrease with excitation energy.

Alternatively, in a sequential decay process the ^{14}Be nucleus must emit one of six possible neutrons to resonant states above the 5n decay threshold (10.3 MeV) in ^{13}Be, rather than to lower energy states. In turn ^{13}Be must decay to resonances above the 4n decay threshold of ^{12}Be. Thus, although there is a factor of 6 enhancement in the number of possible decay paths for the neutron emission, there are 5 intermediate steps in which the system may decay to states below the $\alpha + \alpha + x$n threshold. Moreover, the phase-space at each step is highly constrained. The 6 step sequential emission phase-space is calculated to be at least $\sim 10^3$ times smaller than the direct helium decay process for excitation energies around 15 to 20 MeV.

It is possible that the excitation mechanisms leading to the first-chance He-cluster breakup and neutron removal are radically different. Certainly, direct elastic breakup and absorptive processes dominate in the first step over resonant breakup as they have been used extensively to determine the ground state structure of neutron-rich nuclei [1]. It is thus probable that a fraction of the $\alpha + \alpha + 6$n yield for ^{14}Be is produced via such processes.
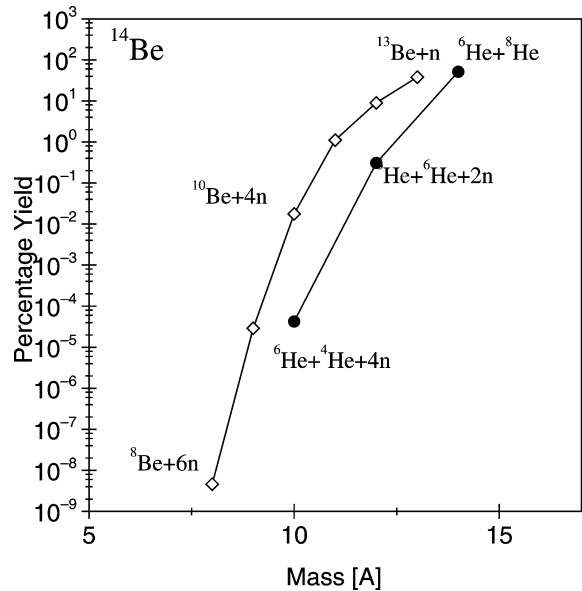

Fig. 5. The calculated percentage yields for neutron decay channels ^{13}Be + n to ^{8}Be + 6n (2 to 7 body decay phase-space) (diamonds) and helium breakup channels (circles) ^{6}He + ^{8}He, ^{6}He + ^{6}He + 2n, ^{6}He + ^{4}He + 4n (2, 4 and 6 body decay phase-space) for the breakup of ^{14}Be at an excitation energy of 20 MeV, using the Fermi breakup model (see the main text for details).

The measurements presented here provide evidence for the existence of di-cluster structures in $^{10-12,14}$Be. Certainly, if the breakup process samples the overlap between the wavefunctions of the ground state and the excited states, the first-chance cluster breakup cross-sections, shown in Fig. 4(a), indicate that the

^{x}He $+$ $^{A-x}$He cluster structure does not decrease over the mass range $A = 10$, 12 and 14. Given also that the decay energy threshold increases with mass number, the present data may even indicate a slight increase in clustering. The breakup cross-sections also appear to demonstrate that these nuclei possess a stronger structural overlap with an $\alpha - X$n$-\alpha$ configuration, although the reaction mechanics by which this final state is reached may be complex. That is to say that the dominant structural mode of the neutron rich isotopes may be identified with two alpha-particles plus valence neutrons. These comprehensive measurements of the neutron-removal and cluster breakup for the first time provide experimental data whereby the structure of the most neutron-rich Be isotopes can be modeled via their reactions.

Acknowledgements

References

[1] P.G. Hansen, A.S. Jensen, B. Jonson, Annu. Rev. Nucl. Part. Sci. 45 (1995) 591.
[2] H. Horiuchi, in: Proceedings of the 7th International Conference, Clustering Aspects of Nuclear Structure and Dynamics, World Scientific, Singapore, 2000, p. 405.
[3] K. Ikeda, N. Tagikawa, H. Horiuchi, Prog. Theor. Phys. Jpn. (Suppl. Extra Number) (1968) 464.
[4] B. Buck, H. Friedrich, C. Wheatley, Nucl. Phys. A 275 (1977) 246.
[5] J. Hiura, R. Tamagaki, Prog. Theor. Phys. Suppl. 52 (1972) 25.
[6] W. von Oertzen, Z. Phys. A 357 (1997) 355.
[7] N. Itagaki, S. Okabe, Phys. Rev. C 61 (2000) 044306.
[8] Y. Kanada-En'yo, H. Horiuchi, A. Doté, Phys. Rev. C 60 (1999) 064304;
A. Doté, H. Horiuchi, Y. Kanada-En'yo, Phys. Rev. C 56 (1997) 1844.
[9] Y. Kanada-En'yo, H. Horiuchi, A. Ono, Phys. Rev. C 52 (1995) 628.
[10] Y. Kanada-En'yo, H. Horiuchi, Phys. Rev. C 52 (1995) 647.
[11] M. Freer, et al., Phys. Rev. Lett. 82 (1999) 1383.
[12] H. Takemoto, H. Horiuchi, A. Ono, Phys. Rev. C 63 (2001) 034615.
[13] F.M. Marqués, et al., Phys. Rev. C 65 (2002) 044006.
[14] M. Labiche, Ph.D. Thesis, Laboratoire de Physique Corpusculaire, 1999, unpublished.
[15] M. Labiche, et al., Phys. Rev. Lett. 86 (2001) 600.
[16] R. Anne, et al., Nucl. Phys. A 575 (1994) 124.
[17] A. Navin, et al., Phys. Rev. Lett. 85 (2000) 266.
[18] M. Freer, et al., Phys. Rev. C 63 (2001) 034301.
[19] Y. Kanada-En'yo, H. Horiuchi, Phys. Rev. C 68 (2003) 014319.
[20] E. Fermi, Theor. Phys. 5 (1950) 1570.
[21] M. Kretschmar, Annu. Rev. Nucl. Sci. 11 (1961) 1.
[22] M. Epherre, E. Gradsztajn, J. Phys. (Paris) 18 (1967) 48.